



RESEARCH ARTICLE

# Morpho-anatomical responses of *Catharanthus roseus* (L.) G.Don due to combined heavy metal stress observed under Scanning Electron Microscope

V. Soumya, P. Kiranmayi\* & K. Siva Kumar

Department of Biotechnology, Gandhi Institute of Technology and Management (Deemed to be University), Visakhapatnam 530 045, India

\*Email: [kpatnala@gitam.edu](mailto:kpatnala@gitam.edu)



## ARTICLE HISTORY

Received: 09 December 2021

Accepted: 16 April 2022

Available online

Version 1.0: 13 May 2022

Version 2.0: 01 July 2022



## Additional information

**Peer review:** Publisher thanks Sectional Editor and the other anonymous reviewers for their contribution to the peer review of this work.

**Reprints & permissions information** is available at [https://horizonepublishing.com/journals/index.php/PST/open\\_access\\_policy](https://horizonepublishing.com/journals/index.php/PST/open_access_policy)

**Publisher's Note:** Horizon e-Publishing Group remains neutral with regard to jurisdictional claims in published maps and institutional affiliations.

**Indexing:** Plant Science Today, published by Horizon e-Publishing Group, is covered by Scopus, Web of Science, BIOSIS Previews, Clarivate Analytics, etc. See [https://horizonepublishing.com/journals/index.php/PST/indexing\\_abstracting](https://horizonepublishing.com/journals/index.php/PST/indexing_abstracting)

**Copyright:** © The Author(s). This is an open-access article distributed under the terms of the Creative Commons Attribution License, which permits unrestricted use, distribution and reproduction in any medium, provided the original author and source are credited (<https://creativecommons.org/licenses/by/4.0/>)

## CITE THIS ARTICLE

Soumya V, Kiranmayi P, Kumar K.S. Morpho-anatomical responses of *Catharanthus roseus* due to combined heavy metal stress observed under Scanning Electron Microscope. Plant Science Today. 2022; 9(3): 623–631. <https://doi.org/10.14719/pst.1621>

## Abstract

Heavy metals trigger various plant responses that basically vary with the intensity as well as duration of stress. Comprehension of the morphological and anatomical responses to such stress is essential for a holistic perception of plant resistance mechanisms to metal-excess conditions in higher plants. In the present study, the effects of heavy metals on morpho-anatomy of *Catharanthus roseus* (L.) G.Don based on its potential to tolerate metal stress has been studied in industrially polluted environments. The tissue samples of these plants grown in contaminated and uncontaminated soils were processed for analysis under Scanning Electron Microscope (SEM). Briefly, harvested tissues were pre-fixed using glutaraldehyde and paraformaldehyde in sodium cacodylate (CAC) buffer, followed by post fixation in osmium tetroxide. Further, the digital micrographs of critically dried samples were captured. The analysis of micrographs revealed structural changes like cell wall thickening, increased stele diameter, increased root and shoot diameter, variations in stomatal number, enlargement of trichomes and salt glands of plants grown in contaminated soil when compared to those grown in uncontaminated soil. The study also provided microscopic evidence of endophytic colonization of microorganisms within surface-disinfected plant tissues. Based on the varied morpho-anatomical responses due to heavy metal stress, several physiological and metabolic mechanisms of plants were deciphered.

## Keywords

*Catharanthus roseus*, industrial soil, heavy metals, micrographs, morphology, SEM

## Introduction

Heavy metal stress triggers several plant responses. Plant reactions exist to circumvent the potential effects caused by a wide range of heavy metals. Heavy metals such as iron, copper, nickel, cobalt, cadmium, zinc, arsenic and mercury are for long being amassed in soils near industrial areas. Most of these metals are essential micronutrients that control several regular processes in plants. However, excess of these metals can elicit varied morpho-anatomical responses in plants (1). Tolerance to metal stress is an intricate parameter in which performance of a plant can be influenced by several characteristics that are important for plant–water relationships (2), root-shoot elongation, biomass allocation (3), seed germination and hydraulic or stomatal conductance (4, 5). While several plant species were known to exhibit decreased growth, several others exhibited enhanced growth and metabolism under metal excess conditions (6). The responses of plants to metal

stress generally alter with the intensity as well as with the period of stress. However, plants' responses to a combination of metal stress cannot be deduced from their responses to the individual metal stress (7).

Comprehending the morphological and physiological responses of plants to metal stress is essential for a holistic perception of resistance mechanisms against metal excess conditions. According to our previous research *Catharanthus roseus* (L.) G. Don when grown in industrially polluted soils for 6 months exhibited altered accumulation of several phytochemicals that were responsible for plant's stress resistance. These plants also showed increased antioxidant potential and photosynthetic activity when compared to plants that were grown in uncontaminated soil (Unpublished). The results indicated that not only plants could withstand the metal stress up to the level tested, but they could probably also utilize these metals in their physiological processes. In the present study however, the effects of heavy metals on plant morphoanatomy based on its ability to tolerate metal stress has been studied in industrially contaminated environments. Soil samples collected from Hindustan Shipyard Limited i.e., HSL (Visakhapatnam city-India) and garden of Gandhi Institute of Technology and Management (Visakhapatnam city-India) were chosen as the test and control respectively based on the concentration level of few tested metals present in the soil (8). Fig. 1A depicts the difference between the concentrations of various metals present in the test and control soil.

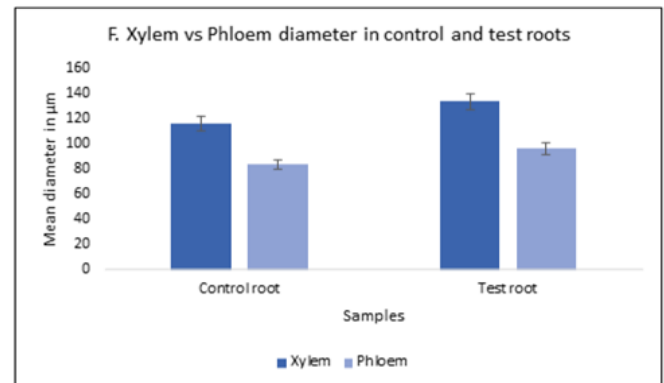
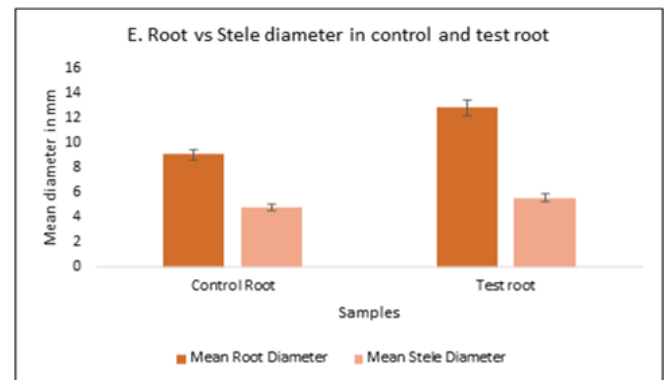
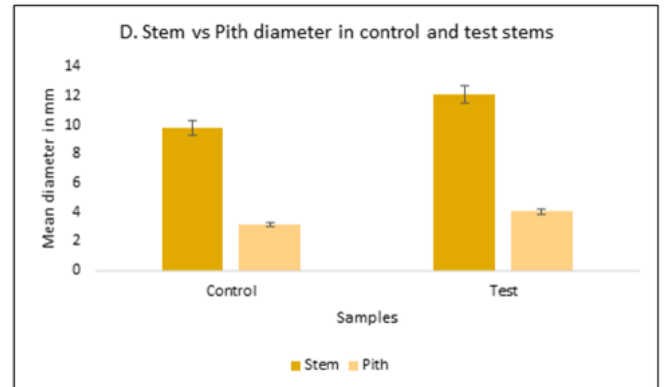
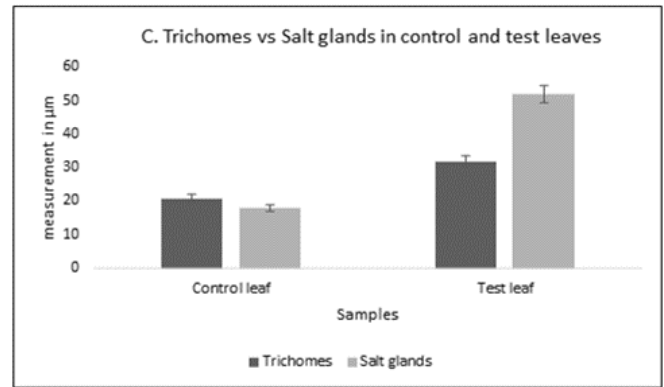
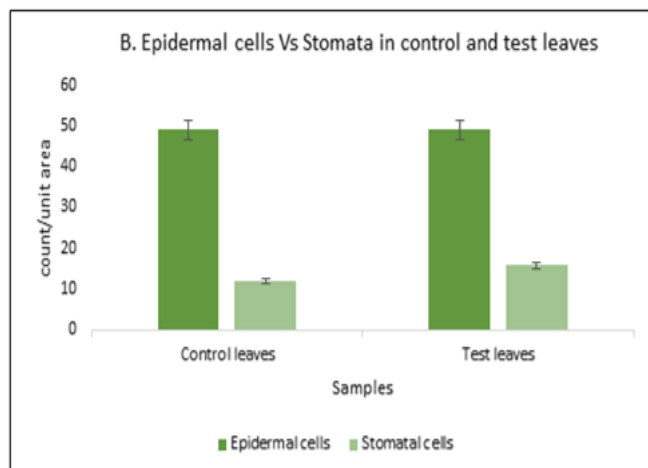
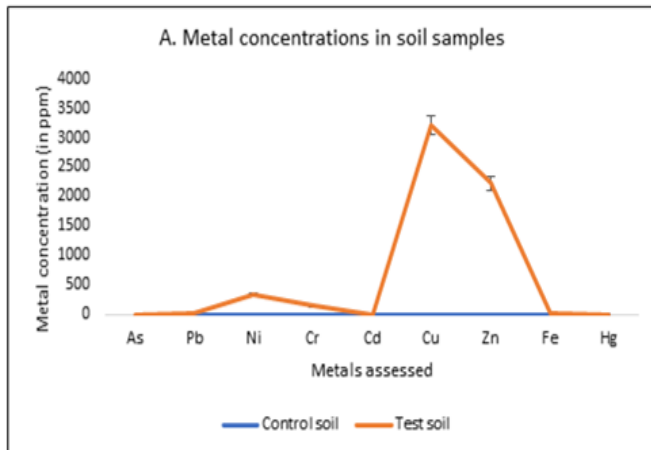


**Fig. 1.** Soil heavy metal concentrations and responses of *Catharanthus roseus* to heavy metal stress. (A): Metal concentrations in soil samples. The heavy metal concentrations were analysed via Atomic Absorption Spectrometric method (8). The test soil had very high concentrations of metals especially copper and zinc in comparison to control soil. Arsenic and Mercury are less than 0.5 ppm (B): Number of epidermal cells and stomata in control and test leaves. There was 33% increase in stomatal number per unit area in the test sample when compared to control sample. However, the number of epidermal cells per unit area showed did not vary. (C): Variations in trichomes and salt glands in control and test leaves. The mean length of trichomes and salt glands was 52% and 188% greater in test sample when compared to control sample. (D): Variations in diameter of stem and pith in control and test samples. The stems were 23% thicker with 28% greater extent of pith in test plants than the control plants. (E): Variations in root and stele diameter in control and test roots. The test roots were 41.7% thicker having 16.6% larger stele diameter than control roots. (F): Variations in xylem and phloem diameters in control and test roots. The mean diameter of xylem and phloem were 14.5% and 15.4% greater in test roots than control roots respectively.

## Materials and Methods

### Physicochemical properties of soil

Physicochemical properties of soil samples like pH, electrical conductance, organic matter, particle size and moisture were also analyzed and reported as Table 1. Acid digestion was done using the aquaregia digestion method for measuring 'total' trace elements in the soil (8). To 1g of each soil sample 1.5 ml hydrogen peroxide, 4.5 ml hydrochloric acid and 1.5 ml nitric acid were added. Hydrogen peroxide was used to enhance the degradation of organic matter in the soil. The digestion was carried out on an electric hot plate. After the process, each aliquot of digested sample was diluted to 100 ml with Milli-Q water and analyzed by Atomic Absorbance Spectrophotometry.

**Table 1.** Physicochemical properties of contaminated soil samples. The samples were slightly basic in nature, with electrical conductivity between 0.1 to 0.3 (8)

Physicochemical parameters	Garden	HSL
pH	7.78	7.47
Electrical conductivity (EC)	0.29	0.11
Organic matter(OM-LOI %)	17.6	5.9
Sand %	13	33
Silt %	69	58
Clay %	12	3
Gravel %	6	16
Moisture (MC%, MF)	17.508, 1.175	7.009, 1.070
<b>Metal (in ppm)</b>		
Lead	9.8	33.41
Nickel	11.0	348.78
Chromium	12.4	142.73
Cadmium	1.4	6.5
Copper	17.8	3187
Zinc	14.0	2218
Iron	16.1	249.1

### Plant growth and environmental conditioning

20 days old *Catharanthus roseus* (L.) G. Don seedlings were obtained from nursery of Gandhi Institute of Technology and Management and planted into each soil type in sets of three. Seedlings were misted wet and placed at 37 °C in a dark room for 2 days. Later, the seedlings were allowed to grow for 6 months, during which the soil temperature and humidity was maintained at 68 F and 40% respectively. Seedlings were exposed to light intensity (above 2100 Candela steradian/ square meter) and adequate air movement. Periodic scouting was done to maintain accurate soil moisture throughout the growth period.

### Sample processing

The tissue samples (leaf, stem and root) of 6 months old *Catharanthus roseus* grown in test and control soil were harvested and processed immediately. The samples were pre-fixed in glutaraldehyde (3.5%) and paraformaldehyde (2%) in 0.1 M sodium cacodylate (CAC) buffer (pH 7.2) for 4 hr at room temperature (9). Samples were post-fixed in osmium tetroxide (0.1% w/v) in CAC buffer for 2 hr at room

temperature. After fixation, the samples were washed with distilled water followed by dehydration using graded ethanol series (20%, 40%, 60%, 70%, 80%, 90% and 99%) of 10 min for each ethanol concentration (10). Samples were eventually dried in a critical point dryer (Agar Scientific Ltd.) with liquid CO<sub>2</sub> and mounted on SEM stubs before being coated with gold (200 Angstroms) using an Emitech K550X sputter coater (Quorum Technologies). Observation of tissues was done using Philips XL30 Scanning Electron Microscope (SEM) that was operated at 10 kV for capturing the digital micrographs.

## Results and Discussion

Growth being one of the most important physiological processes is generally linked to nutrient uptake efficiency of the plant. The plants grown in soil collected from HSL showed increased height, thicker shoot and root system, deeper root penetration, larger leaves and enhanced chlorophyll content when compared to plants grown in control soil. The anatomical alterations that occurred in leaves, stems and roots of plants grown in industrial soil were assessed based on SEM micrographs. The micrographs were analysed using ImageJ software (11).

### Analysis of leaf micrographs

The control and test leaf micrographs are shown in Fig. 2 and Fig. 3. The leaf epidermis constituted a single protective layer of cells that served as a barrier to environmental factors like loss of water, pathogen attack and herbivory (12). Epidermal cells were irregularly shaped throughout the observed leaf micrographs. One of the key characteristics of epidermal cells is the biosynthesis of cuticular wax layer (13). In general, this cuticle layer is extremely hydrophobic. It therefore not only minimizes water loss from the plant but also growth of fungi and bacteria on plant surfaces. The leaf micrographs revealed random distribution of stomata on the entire surface. The test leaf had 33% more stomatal apertures per square unit of leaf epidermis than control leaf as depicted in Fig. 1B. A plant that has high stomatal density generally exhibits high rate of photosynthetic potential. However, the plant controls the photosynthetic rate by managing stomatal aperture as a balancing act between transpiration and carbon dioxide inflow. This is accomplished by physical openings on the plant surface known as guard cells that aid in exchange of gases between plants and the atmosphere (14).

Trichomes in *Catharanthus roseus* were conical in shape with increased mean length by 52% in the test leaves than control leaves. Trichomes are known to have protective roles in plants. They act as protectors against pests, aid in conservation of heat and moisture. They are the sites for secondary metabolite production in plants. Trichome number within plants is generally regulated by same factors that affect the stomatal number (15). The leaves had salt gland like structures which apparently served as reservoirs of excreted metal (16). The micrographs of test leaf revealed glands that were strikingly larger (188%) than those in control leaf. Such glands aid in

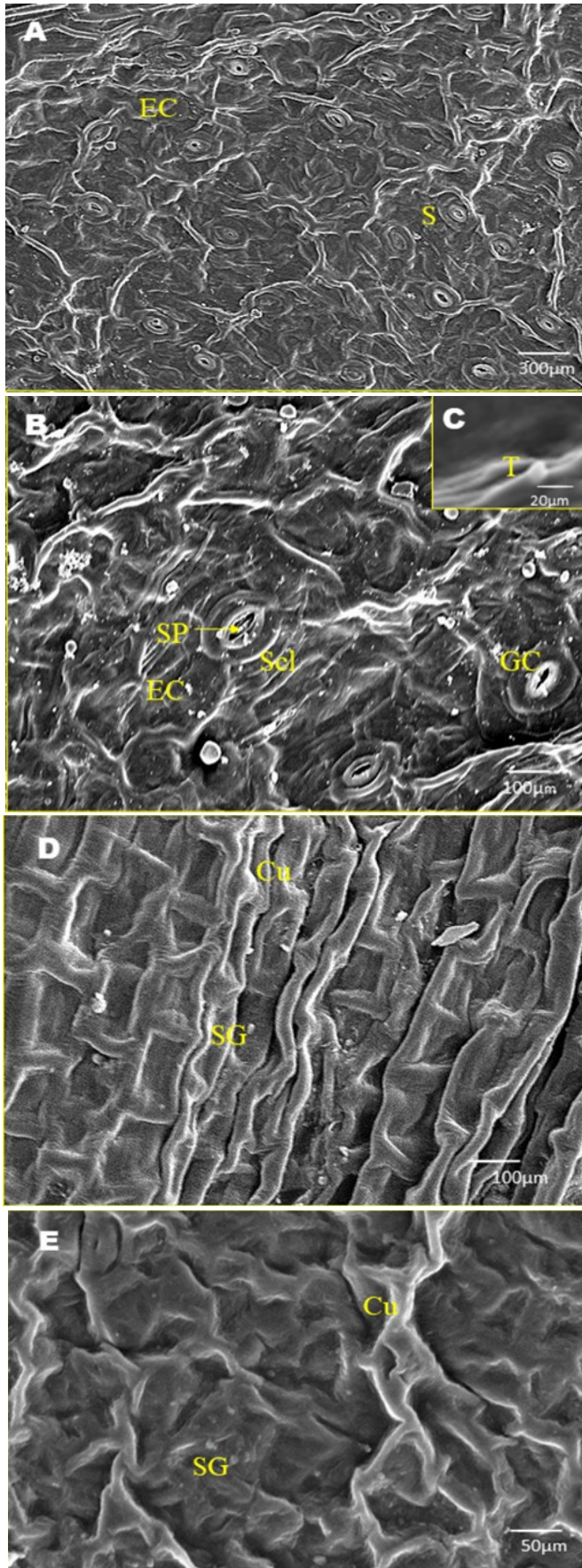


**Fig. 2.** Leaf micrographs of *Catharanthus roseus* grown in uncontaminated soil- Control leaf. (A): The leaf epidermal layer. EC, Epidermal cells; S, Stomata; Scale bar is 300  $\mu\text{m}$ . (B): Leaf epidermis showing irregularly shaped epidermal cells. SP, Stomatal opening; GC, Guard cells; Scl, Sclerenchyma cells; Scale bar is 100  $\mu\text{m}$ . (C): Trichomes magnification showing its conical shape. T, Trichome; Scale bar is 20  $\mu\text{m}$ . (D): Leaf tissue showing cuticle wax deposition and salt glands. Cu, Cuticle; SG, Salt glands. Scale bar is 100  $\mu\text{m}$ . (E): Cuticle and salt glands at higher magnification. Scale bar is 50  $\mu\text{m}$ .

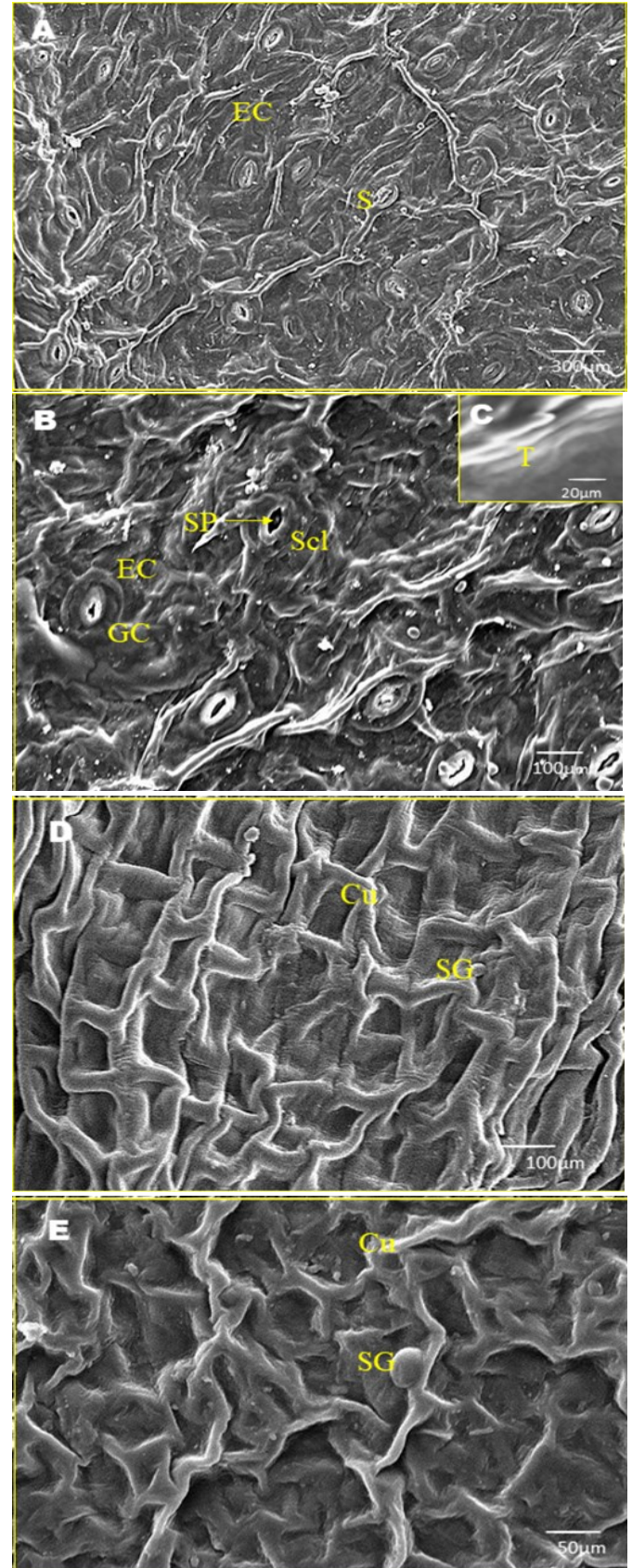


**Fig. 3.** Leaf micrographs of *Catharanthus roseus* grown in contaminated soil- Test leaf. (A): The leaf epidermal layer. EC, Epidermal cells; S, Stomata; Scale bar is 300  $\mu\text{m}$ . (B): Leaf epidermis showing irregularly shaped epidermal cells. SP, Stomatal opening; GC, Guard cells; Scl, Sclerenchyma cells; Appearance of more number of stomata when compared to Fig. 2(B) Scale bar is 100  $\mu\text{m}$ . (C): Trichomes magnification showing its conical shape. T, Trichome; Trichomes were larger than control leaf Fig. 2(C). Scale bar is 20  $\mu\text{m}$ . (D): Leaf tissue showing cuticle wax deposition and salt glands. Cu, Cuticle; SG, Salt glands. Scale bar is 100  $\mu\text{m}$ . (E): Cuticle and salt glands at higher magnification. Salt glands were strikingly larger in test leaf in comparison to control leaf Fig. 2(E). Scale bar is 50  $\mu\text{m}$ .

transfer the surplus of heavy metals to the outside by the plant (17). However, further studies should be carried out in order to understand the mechanism behind formation of such glands (Fig. 1C).

#### Analysis of stem micrographs

The micrographs of stem transverse sections revealed several anatomical changes that occurred during plant growth in industrial soil (Fig. 4 and Fig. 5).

The stem diameter increased by 23% in test sample than control stem sample. Pith was the prominent central part of the stem composed of parenchymatous cells which enclosed intercellular spaces. The test plants had 28% larger mean pith diameter than the control plants (Fig. 1D).

The parenchymatous cells in pith stored food and helped in transporting nutrients throughout the plant. The extent of cortex in the test sample was also greater than

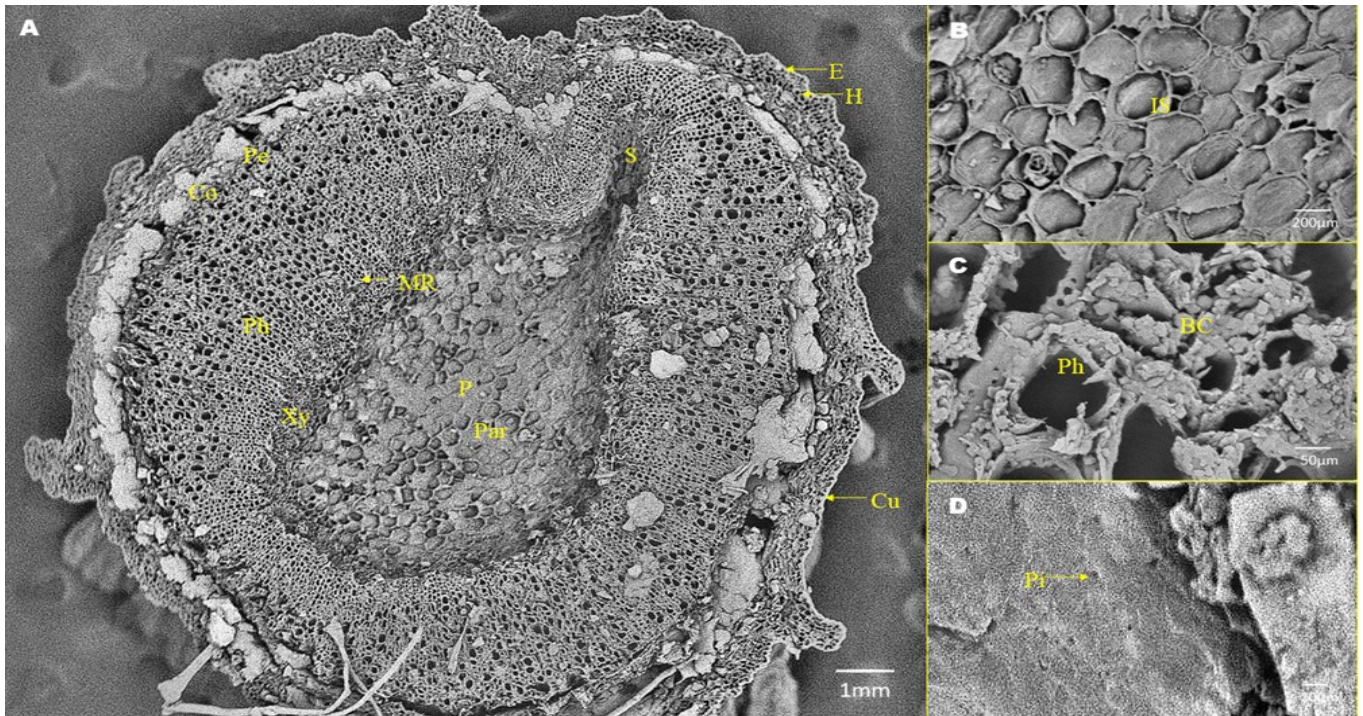


**Fig. 4.** Stem micrographs of *Catharanthus roseus* grown in uncontaminated soil- Control stem. (A): The stem cross section of control plant. Cu, Cuticle; E, Epidermis; H, Hypodermis; P, Pith; Par, Parenchyma; Xy, Xylem; Ph, Phloem; MR, Medullary ray; Pe, Pericycle; Co, Cortex; Scale bar is 1000 µm. (B): Parenchyma of pith. IS, Intracellular spaces; Scale bar is 200 µm. (C): Vessels revealing endophytes. Ph, Phloem; BC, Endophytic bacterial colonies; Scale bar is 50 µm. (D): the walls of vessels showing pits. Pi, Pits; Scale bar is 20 µm

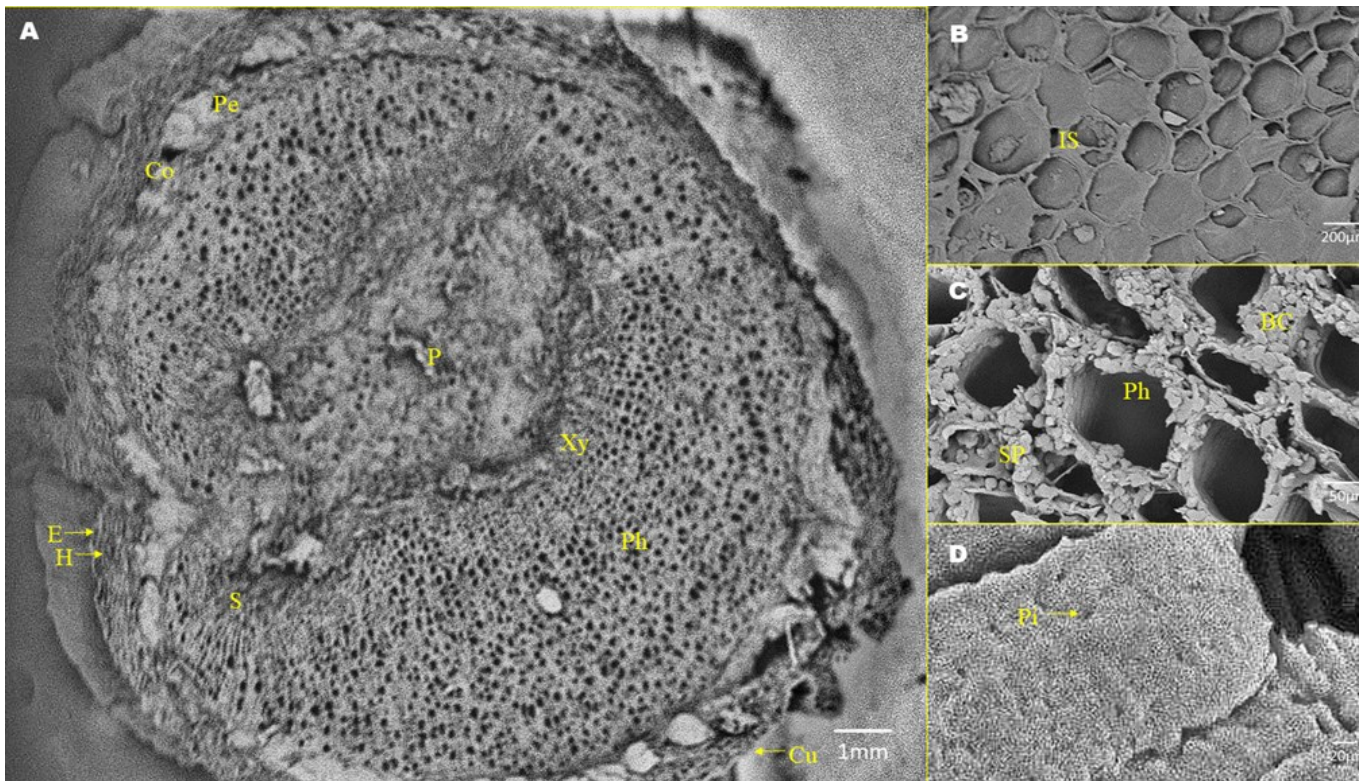


**Fig. 5.** Stem micrographs of *Catharanthus roseus* grown in contaminated soil- Test stem. (A): The stem cross section of test plant. Cu, Cuticle; E, Epidermis; H, Hypodermis; P, Pith; Xy, Xylem; Ph, Phloem; Pe, Pericycle; Co, Cortex; Scale bar is 1000 µm. (B): Parenchyma of pith. IS, Intracellular spaces; Scale bar is 200 µm. (C): Vessels revealing endophytes. BC, Endophytic bacterial colonies; SP, Sieve plate; Ph, Phloem; the diameter of phloem was larger in test sample than in control. Scale bar is 50 µm. (D): the walls of vessels showing pits. Pi, Pits; Scale bar is 20 µm.

the control sample. It was made up of thin walled angular parenchymatous cells that enclosed intercellular spaces. The major function of the cortex was to store food (18). The medullary rays connected the pith with pericycle and cortex. These radial strips were polygonal parenchymatous cells with small intercellular spaces. The cells made intimate contact with the conducting cells of both phloem and xylem through pits and help in the radial conduction of food and water.

The phloem and xylem cells were differentiated from the cambium layer. Phloem tissue is composed of sieve tubes and companion cells. It transports the manufactured carbohydrates downward in plant stems. The phloem vessel diameter was quite conserved in test and control samples. Sieve plate, which is the perforated end wall of a sieve tube, is seen in Fig. 5(C). Xylem walls were heavily lignified in test samples. Lignification of xylem allows it to withstand alterations in pressure as water moves throughout the plant. However, the mechanisms controlling the spatial deposition of lignin remains unclear. The xylem cells were more than inert tubes. These sophisticated systems regulate and conduct water to those areas of a plant that need water the most (19). This preferential water conduction involved the direction of water molecules through pits in adjacent cell walls observed in test as well as control samples Fig. 4(D) and Fig. 5(D).

The pits composed of cellulose and pectin were observed in the micrographs. The pit diameter dynamically influences the membrane hydraulic resistance and its capacity to limit the coagulum between the conduits. The control of water movement involves pectin hydrogels that

aid in keeping the adjacent cell walls together. When pectin swells due to imbibition, pore size gets reduced, slowing the water flow. Similarly, the pores open wide when the pectin shrink and enable the water to flush across the xylem towards the leaves. This exceptional control of water movement might allow the plant to respond to abiotic stress conditions.

The cuticle appeared as a layer outside the epidermis of the stem. It played a crucial role in the adaptation of plants to abiotic stress by delaying the damage of plants from environmental stress (20). Studies suggest that the permeability of cuticle depends on wax constitution rather than the total wax load in plants (21).

#### Analysis of root micrographs

Mean root diameter varied considerably between test and control samples indicating 41.7% thicker root system in plants grown in industrial soil. Fig. 6 and Fig. 7. The healthy growth of plants was indicative that the root radius influenced nutrient uptake by plants growing in soil. Micrographs suggest that the mean diameter of cortical cells did not change between the two root samples, instead mean stele diameter (xylem and phloem together) of test roots increased by 16.6%, indicating significant contribution of stele in increasing root diameter of test plants (Fig. 1E.)

The mean vessel diameter in test root was larger than in control root. Test root showed 14.5% and 15.4% increase in the diameter of xylem and phloem respectively. This showed their association with a pronounced radial and greater root interception for nutrient uptake in test samples. Fig. 1F. The crenulated appearance of the phloem

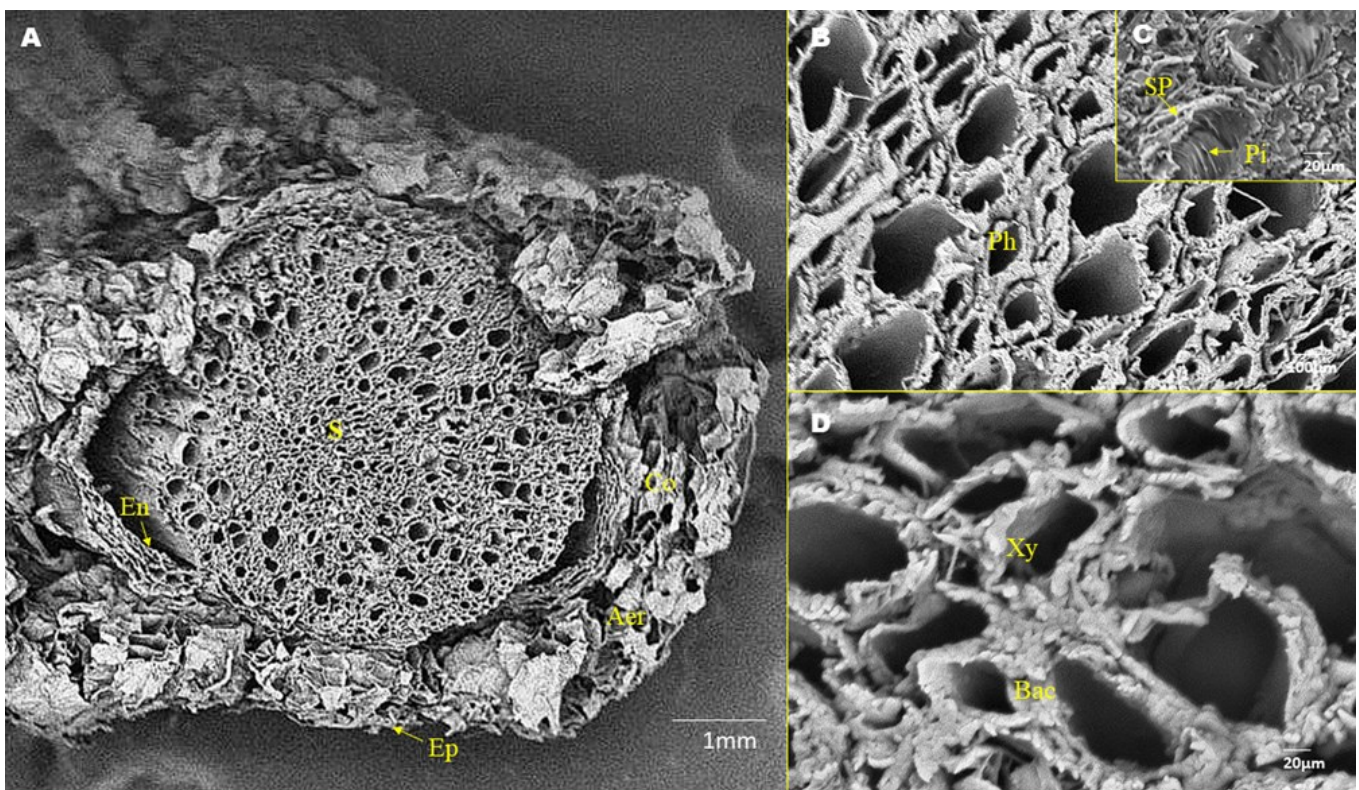


**Fig. 6.** Root micrographs of *Catharanthus roseus* grown in uncontaminated soil- Control root. (A): The root cross section of control plant. S, Stele; En, Endodermis; Co, Cortex; Aer, Aerenchyma; Ep, Epidermis; the cortex was seen collapsed perhaps during sample dehydration steps. Scale bar is 1000  $\mu\text{m}$ . (B): Root stele. Scale bar is 100  $\mu\text{m}$ . (C): Vessels revealing pits and sieve plates. Ph, phloem; SP, Sieve plate; Pi, pits; Scale bar is 20  $\mu\text{m}$ . (D): Vessels revealing endophytes. Xy, Xylem; Bac, Endophytic bacteria; Scale bar is 20  $\mu\text{m}$ .

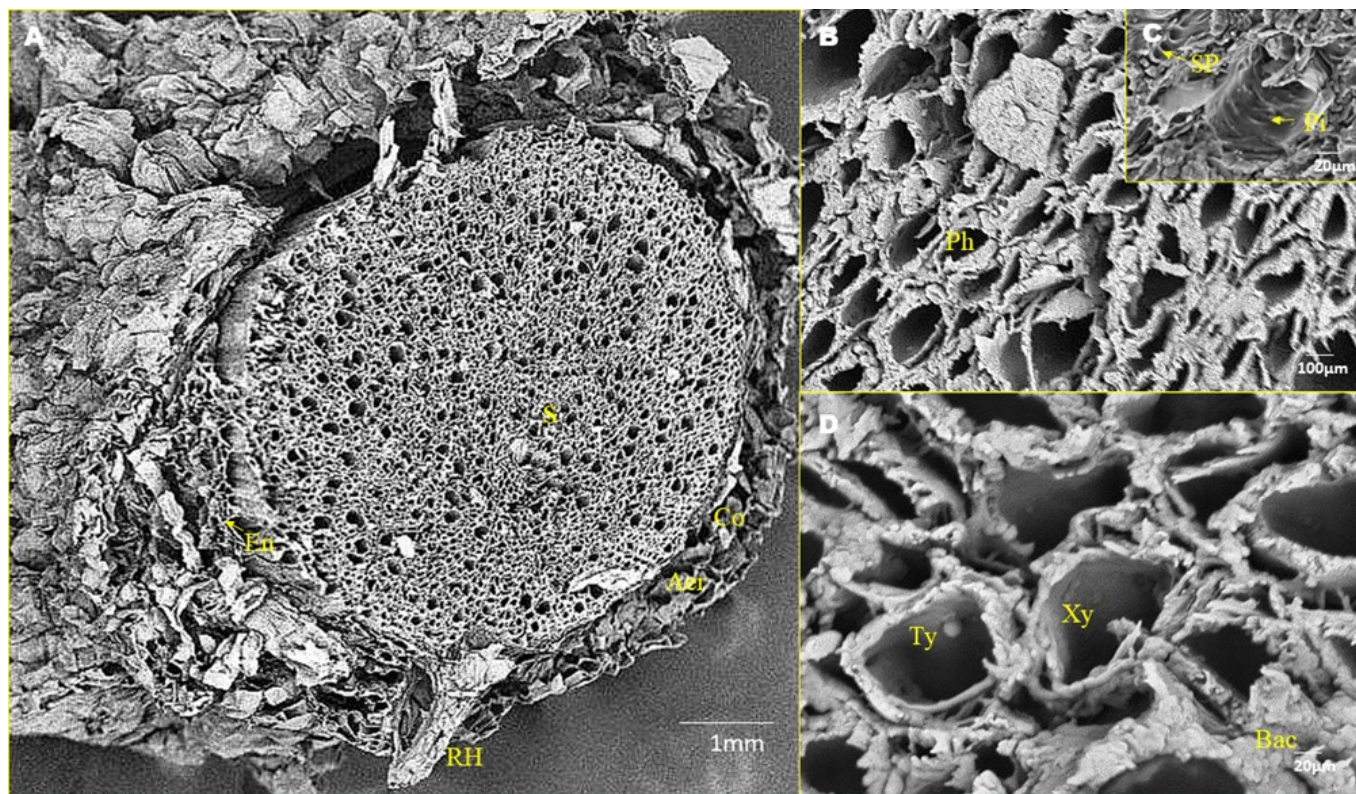


**Fig. 7.** Root micrographs of *Catharanthus roseus* grown in contaminated soil- Test root. (A): The root cross section of control plant. S, Stele; En, Endodermis; Co, Cortex; Aer, Aerenchyma; Ep, Epidermis; RH, Root hair; the cortex was seen collapsed to a larger extent than in control root Figure 9(A). Scale bar is 1000  $\mu\text{m}$ . (B): Root stele. Scale bar is 100  $\mu\text{m}$ . (C): Transverse section of vessels revealing pits and sieve plates. Ph, phloem; SP, Sieve plate; Pi, pits; Scale bar is 20  $\mu\text{m}$ . (D): Vessels revealing Tyloses and endophytes. Xy, Xylem; Bac, Endophytic bacteria; Ty, Tyloses. Scale bar is 20  $\mu\text{m}$ .

end walls suggested formation of sieve elements giving rise to sieve plates from the transverse walls of these young sieve elements.

Aerenchyma is a tissue that is characterized by continuous gas spaces (22). It is located in the cortex region. The structural features of aerenchyma were same whether the plants grew in test soil or control soil. The presence of the large cells of aerenchyma provide a pathway for the diffusion of oxygen from the aerial parts of the plant to roots (23). Rhizodermis and exodermis were seen collapsed in the test and control samples perhaps during dehydration steps while processing the sample. However, the extent of collapse was larger in test root than the control root probably due to metal toxicity.

Tyloses like structures were observed in the xylem vessels of test root. Tyloses are the protoplasmic outgrowths of parenchymatous cells that protrude out through pits into the xylem vessels. They generally form within xylem vessels in response to several abiotic and biotic stress (24). However, further biochemical and anatomical study should be undertaken to confirm these structures in *Catharanthus roseus*.

Plants face metal toxicity during their entire period of growth. However, most of the plant species become adaptable to stressed conditions and exhibit healthy growth even while growing under high levels of soil metals (25). Plants adopt various mechanisms to deal with such environmental stress, for instance, (a) plants can keep metal ions from entering into their cells; (b) plants can absorb high concentrations of metals and allocate them in their organs/tissues (c) plants can detoxify the metals so that there is no disruption in plant growth (25).

The heavy metal stress in plants can affect the plants metabolism leading to several structural and physiological changes (26). Structural changes like lignin formation and thickening of cell walls are among the cellular responses to heavy metal stress. Other phenomena like increase in the number and size of vessels in plants could also be detected under the metal stressed conditions. Our previous research on *Catharanthus roseus* served as a validation exhibiting enhanced photosynthetic activity, elevated chlorophyll, lignin and pectin content under metal stress. (Unpublished). When the root diameter and vascular density increases, it offers more benefits to physiological functions of the roots including improved nutrient transport and water uptake (27). The endophytic colonization of microorganisms within surface-disinfected plant tissues was also observed in this study. Endophytes are interesting group of organisms that inhabit various plant tissues without causing any apparent plant diseases. Studies on endophytic alterations within metal stressed plants could provide a better prediction of their interactions with the host.

## Conclusion

Our investigation revealed the effects of combined metal stress on morpho-anatomy of *Catharanthus roseus* (L.) G.Don. Briefly, the data indicated that the increase of soil heavy metals induced *Catharanthus roseus* to produce a higher number of stomata, enlarged trichomes and glands, increased vessel dimensions and larger diameter of roots and shoots. Our work demonstrated the ample morpho-anatomical differences in leaves, stems and roots of *Catharanthus roseus* grown in contaminated and uncon-

taminated soils.

## Acknowledgements

The authors acknowledge Department of Biotechnology, Institute of Science, Gandhi Institute of Technology and Management (Deemed to be University) – Visakhapatnam, for its support in carrying out this work. The authors appreciate the technical support received from Dr. D. Harinarayana, Nishka Laboratory (Hyderabad) in handling the Scanning Electron Microscope.

## Authors contributions

VS was involved in maintenance of plants' growth, carried out the analysis of micrographs and drafted the manuscript. The conceptualization and supervision of experiments was carried out by PK. KSK assisted in analysis of the micrographs. All authors read and approved the final manuscript.

## Compliance with ethical standards

**Conflict of interest:** Authors do not have any conflict of interests to declare.

**Ethical issues:** None

## References

1. Tatiana M, Grigoriy F, Dina N, Aleksei F, Victor C, Saglara M. Morphological and anatomical changes of *Phragmites australis* Cav. due to the uptake and accumulation of heavy metals from polluted soils. *Science of The Total Environment*. 2018;636:392-401. <https://doi.org/10.1016/j.scitotenv.2018.04.306>.
2. Vahid T. Interactive effects of zinc and boron on growth, photosynthesis and water relations in pistachio. *Journal of Plant Nutrition*. 2017;40(11):1588-1603. <https://doi.org/10.1080/01904167.2016.1270308>
3. Xinyi C, Mingyan J, Jiarong L, Yixiong Y, Ningfeng L, Qibing C et al. Biomass allocation strategies and Pb-enrichment characteristics of six dwarf bamboos under soil Pb stress. *Ecotoxicology and Environmental Safety*. 2021;207:111500. <https://doi.org/10.1016/j.ecoenv.2020.111500>.
4. Laura YE, Roberto BG, Joel F, Elizabeth AC. Effect of heavy metals on seed germination and seedling development of *Nama aff. stenophylla* collected on the slope of a mine tailing dump. *International Journal of Phytoremediation*. 2020;22(14):1448-61. <https://doi.org/10.1080/15226514.2020.1781782>
5. Fernandez DM, Walker DJ, Espinar PR, Flores P, Río JA. Physiological responses of *Bituminaria bituminosa* to heavy metals. *Journal of Plant Physiology*. 2011;168(18):2206-11. <https://doi.org/10.1016/j.jplph.2011.08.008>.
6. Disante KB, Fuentes D, Cortina J. Response to drought of Zn-stressed *Quercus suber* L. seedlings. *Environmental and Experimental Botany*. 2011;70(2-3):96-103. <https://doi.org/10.1016/j.envexpbot.2010.08.008>.
7. Mittler R. Abiotic stress, the field environment and stress combination. *Trends in Plant Science*. 2006;11(1):15-19. <https://doi.org/10.1016/j.tplants.2005.11.002>.
8. Soumya V, Sowjanya A, Kiranmayi P. Evaluating the status of phytochemicals within *Catharanthus roseus* due to higher metal stress. *International Journal of Phytoremediation*. 2021;23(13):1391-1400. <https://doi.org/10.1080/15226514.2021.1900063>
9. Pathan AK, Bond J, Gaskin RE. Sample preparation for scanning electron microscopy of plant surfaces—Horses for courses. *Micron*. 2008;39(8):1049-61. <https://doi.org/10.1016/j.micron.2008.05.006>.
10. Asma A, Wajid Z, Fazal U, Saddam S, Shayan J, Saraj B, Abdul S, Bushra A. Systematics study through scanning electron microscopy; a tool for the authentication of herbal drug *Mentha suaveolens* Ehrh. *Microscopy Research and Technique*. 2020;83(1):81-87. <https://doi.org/10.1002/jemt.23391>
11. Schneider C, Rasband W, Eliceiri K. NIH Image to ImageJ: 25 years of image analysis. *Nat Methods*. 2012;9:671-75. <https://doi.org/10.1038/nmeth.2089>
12. Filotheou HP, Bosabalidis AM, Karataglis S. Effects of Copper Toxicity on Leaves of Oregano (*Origanum vulgare* subsp. *hirtum*). *Annals of Botany*. 2001;88(2):207-14. <https://doi.org/10.1006/anbo.2001.1441>.
13. Vaishali Y, Namira A, Ján K, Vijay PS, Durgesh KT, Devendra KC, Marek V. Structural modifications of plant organs and tissues by metals and metalloids in the environment: A review. *Plant Physiology and Biochemistry*. 2021;159:100-12. <https://doi.org/10.1016/j.plaphy.2020.11.047>.
14. Drake PL, Froend RH, Franks PJ. Smaller, faster stomata: scaling of stomatal size, rate of response and stomatal conductance. *Journal of Experimental Botany*. 2013;64(2):495-505. <https://doi.org/10.1093/jxb/ers347>
15. Karabourniotis G, Liakopoulos G, Nikolopoulos D, Bresta P. Protective and defensive roles of non-glandular trichomes against multiple stresses: structure–function coordination. *Journal of Forestry Research*. 2020;31:1-12. <https://doi.org/10.1007/s11676-019-01034-4>
16. Kalsoom B, Aamir S, Usman A, Asad U, Zahoor UH, Brekhna G, Inam Uh, Sunera, Mehrina A. Foliar micromorphology and its role in identification of the Apocynaceae taxa. *Microscopy Research and Technique*. 2020;83(7):755-66. <https://doi.org/10.1002/jemt.23466>
17. Maheshi D, John CL. Making plants break a sweat: the structure, function and evolution of plant salt glands. *Frontiers in Plant Science*. 2017;8:406. <https://doi.org/10.3389/fpls.2017.00406>
18. Castaneda TG, Brown KM, Lynch JP. Reduced root cortical burden improves growth and grain yield under low phosphorus availability in maize. *Plant, Cell and Environment*. 2018;41(7):1579-92. <https://doi.org/10.1111/pce.13197>
19. Rucinska SR. Water relations in plants subjected to heavy metal stresses. *Acta Physiologiae Plantarum*. 2016;38:257. <https://doi.org/10.1007/s11738-016-2277-5>
20. Yeats TH, Rose JK. The formation and function of plant cuticles. *Plant Physiology*. 2013;163:5-20. <https://doi.org/10.1104/pp.113.222737>.
21. Kim H, Choi D, Suh MC. Cuticle ultrastructure, cuticular lipid composition, and gene expression in hypoxia-stressed *Arabidopsis* stems and leaves. *Plant Cell Rep*. 2017;36:815-27. <https://doi.org/10.1007/s00299-017-2112-5>
22. Leite DCC, Grandis A, Tavares EQP, Piovezani AR, Pattathil S, Avci U, Rossini A, Cambler A, DeSouza AP, Hahn MG, Buckeridge MS. Cell wall changes during the formation of aerenchyma in sugarcane roots. *Annals of Botany*. 2017;120(5):693-708. <https://doi.org/10.1093/aob/mcx050>
23. Cuimin G, Min W, Lei D, Yupei C, Zhifeng L, Jun H, Shiwei G. High water uptake ability was associated with root aerenchyma formation in rice: Evidence from local ammonium supply under osmotic stress conditions. *Plant Physiology and Biochemistry*. 2020;150:171-79. <https://doi.org/10.1016/j.plaphy.2020.02.037>.
24. Mahasin AK, Meghma B, Robert AS, Teresa EVS, Subir B. Evidence of simultaneous occurrence of tylosis formation and fungal interaction in a late Cenozoic angiosperm from the east-

- ern Himalaya. Review of Palaeobotany and Palynology. 2018;259:171-84. <https://doi.org/10.1016/j.revpalbo.2018.10.004>
25. Shanying HE, Xiaoe Y, Zhenli HE, Virupax CB. Morphological and Physiological Responses of Plants to Cadmium Toxicity: A Review. *Pedosphere*. 2017;27(3):421-38. [https://doi.org/10.1016/S1002-0160\(17\)60339-4](https://doi.org/10.1016/S1002-0160(17)60339-4).
26. Pugsley MK, Tabrizchi R. The vascular system: An overview of structure and function. *Journal of Pharmacological and Toxicological Methods*. 2000;44(2):333-40. [https://doi.org/10.1016/S1056-8719\(00\)00125-8](https://doi.org/10.1016/S1056-8719(00)00125-8).
27. Bengough AG, Bransby MF, Hans J, McKenna SJ, Roberts TJ, Valentine TA. Root responses to soil physical conditions; growth dynamics from field to cell. *Journal of Experimental Botany*. 2006;57(2):437-47. <https://doi.org/10.1093/jxb/erj003>

§§§